Bus Clamped DTC of Induction Motor with Four Level Hysteresis band Torque Controller

Naresh B, Durga Devi K

Abstract — Conventional method of direct torque control (DTC) of induction motor suffers from high torque and flux ripple. Smaller hysteresis band tolerances were not desirably reduce ripple content, thereby higher order hysteresis band control is desired. The application of bus clamping to inverter improves performance of DTC in the aspects of quick response and less distortion. In this paper four level hysteresis band toque control is proposed for bus clamped direct torque control (DTC) of induction motor. The four level torque control is deservedly operated with duty ratio control and modified switching table is defined to assure bus clamping operation. The duty-cycle adjustment based four level hysteresis band torque controlled bus clamped DTC reduces the ripple content. The performance investigation of induction motor with proposed method is simulated and comparative results are presented

Index Terms — Bus Clamped Direct Torque Control; Torque ripple; Flux Ripple, Induction motor

1 Introduction

Direct torque control (DTC) is becoming popular method of AC motor control today as alternative to field oriented control because of their prominent advantages [2], [3]. The DTC is mainly concerned by the electromechanical torque and flux vested around their tolerance bounds having with required reference values. Thus the control principle of DTC is defined in terms of torque and flux by means of hysteresis band control. Thereby DTC uses error between set and estimated values of flux and torque information and proper voltage vectors are defined for the inverter switching based on the increase or decrease of flux and torque. The theoretical aspects and principle of this control methodology is first proposed by Takahashi et.al in 1986 for their investigations on high performance drives. Many researchers are called Takahashi DTC method as conventional DTC, which employs two hysteresis comparators and a switching table [1], [6]. But conventional DTC method of control causes moderately high torque and flux ripple and suffers from variable switching frequency of operation as well as acoustic noise. Yong Chang Zhang et. al proposed duty ratio control applied to conventional DTC for reduction of ripple, where duty cycle adjustment of the selected active vector is adjusted [4], [5]. Most of duty cycle control methods only focus on the torque performance improvement and fail to take the flux ripple reduction into account. In [7], [8] N Rumzi, et al has replaced hysteresis torque controller with constant switching frequency torque controller for maintaining constant switching frequency and reducing torque ripple. In [9], Yen-shin, et. al has increased zero switching states and/or increasing switching frequency with increased bands in torque hysteresis controller and modified switching table control in order to reduce the torque ripple. In [10], [11], Jun-Koo Kang and Kuo-Kai Shyu have obtained torque ripple theoretical analysis and proposed DTC based on torque ripple minimum condition. But these approaches are not significantly reduces torque and flux ripple.

The main improvement required in conventional DTC method induction motor is to reduce torque ripple and flux ripple which can be achieved by bus clamped operation of inverter [16]. In [17], Bassem Ei Badsi et. al proposed method of bus clamping inverter operation in which one of the pole voltage is clamped DC bus voltage. The authors are introduced bus-clamping to DTC method leads to keep each inverter phase conduction on or off during 60^0 interval in every half cycle of the stator flux vector. The modified switching table is proposed in order to reduce ripple and distortion. Thus bus clamped DTC strategy is not based on fixed modulation time, so a quick response system is obtained, and bus-clamping technique makes the inverter switch frequency reduced, results reduction of the torque ripple reduced [18]. Further, the conventional approach of prescribed bands of hysteresis torque control in DTC can be altered with higher order hysteresis band torque control for more reduction of torque ripple, when it is operated with duty cycle control, which effects on the active time of operation of inverter voltage vectors [13]. By adopting duty cycle control with higher hysteresis band torque control to the bus clamped DTC makes further reduction in torque ripple and flux ripple. In this paper four level torque hysteresis band control of bus clamped DTC is proposed and the performance results are presented. The proposed method of bus clamped DTC as low inverter switching losses, low current harmonic distortion and torque ripple reduction.

2 Mathematical Model of Induction Motor

The implementation of DTC induction motor requires mathematical model of motor referred in stationary frame. The motor control through this reference frame does not require

- *Naresh B is currently working in the deprtmrnt of electrical & electronics engineering at University college of ingineering Kakinada, JNTU University Kakinada, A.P India, PH-+91884 2300845. E-mail: naresh.jntuce@gmail.com*
- *Durga devi K is currently pursuing masters degree in the deprtmrnt of electrical & electronics engineering at University college of ingineering kakinada, JNTU University Kakinada,. A.P India, E-mail: durgadevi.korra@gmail.com*

much transformations and implementation is easier. The d-q axis voltage equations of induction motor are shown in (1) and (2), and state space model of fluxes in terms of impedances is given in (3) [19], [20]. The generalized torque equation of the motor in terms of stator currents and flux linkages is shown in (4) and (5).

$$v_{qs} = R_s i_{qs} + \frac{d\Psi_{qs}}{dt} \tag{1}$$

$$v_{ds} = R_s i_{ds} + \frac{d\Psi_{ds}}{dt} \tag{2}$$

$$\begin{bmatrix} \dot{\Psi}_{qs} \\ \dot{\Psi}_{ds} \\ \dot{\Psi}_{qr} \\ \dot{\Psi}_{dr} \end{bmatrix} = \begin{bmatrix} 0 & \frac{R_s\,\omega_b}{x_{ls}}\left(\frac{x^*_{ml}}{x_{ls}}-1\right) & 0 & \frac{R_s\,\omega_b}{x_{ls}}\left(\frac{x^*_{ml}}{x_{lr}}\right) \\ \frac{R_s\,\omega_b}{x_{ls}}\left(\frac{x^*_{ml}}{x_{ls}}-1\right) & 0 & \frac{R_s\,\omega_b}{x_{ls}}\left(\frac{x^*_{ml}}{x_{lr}}\right) & 0 \\ 0 & \frac{R_r\,\omega_b}{x_{lr}}\left(\frac{x^*_{ml}}{x_{ls}}\right) & -\omega_r & \frac{R_s\,\omega_b}{x_{lr}}\left(\frac{x^*_{ml}}{x_{lr}}-1\right) \\ \frac{R_r\,\omega_b}{x_{lr}}\left(\frac{x^*_{ml}}{x_{ls}}\right) & 0 & \frac{R_s\,\omega_b}{x_{lr}}\left(\frac{x^*_{ml}}{x_{lr}}-1\right) & -\omega_r \end{bmatrix} \begin{bmatrix} \Psi_{qs} \\ \Psi_{ds} \\ \Psi_{qr} \\ \Psi_{dr} \end{bmatrix} + \omega_b \begin{bmatrix} I & \Theta \\ \Theta & \Theta \end{bmatrix} \begin{bmatrix} v_{qs} \\ v_{ds} \\ v_{qr} \\ v_{dr} \end{bmatrix} \tag{3}$$

where,

$$I = \begin{bmatrix} 1 & 0 \\ 0 & 1 \end{bmatrix} \quad and \quad \Theta : 2\times 2 \ null \ matrix$$

$$x^*_{ml} = \frac{1}{\left(\frac{1}{x_m} + \frac{1}{x_{ls}} + \frac{1}{x_{lr}}\right)}$$

ω_b : *motor angular base frequency*

ω_r : *rotor angular speed*

x_{ls} : *stator leakage reactance*

x_{lr} : *rotor leakage reactance*

x_m : *mutual reactance*

Ψ_{ds} : *d – axis stator flux linkage*

Ψ_{qs} : *q – axis stator flux linkage*

Ψ_{dr} : *d – axis rotor flux linkage*

Ψ_{qr} : *q – axis rotor flux linkage*

v_{ds} v_{qs} : *d and q – axis stator voltages*

v_{dr} v_{qr} : *d and q – axis rotor voltages*

and

$$T_e = \frac{3}{2}\left(\frac{P}{2}\right)\frac{L_m}{L_r L_s^{'}}(\vec{\Psi}_S \times \vec{\Psi}_r) \tag{4}$$

$$= \frac{3P}{4}(\Psi_{ds} i_{qs} - \Psi_{qs} i_{ds}) \tag{5}$$

3 Direct Torque Control of Induction Motor

Rewriting the equation (1) and (2), the stator flux of the induction motor is estimated by integrating stator voltage by deducting winding voltage drop across R_s, which is given in (6) [1], [2]. When the motor is working at its nominal voltage, resistive drop can be ignored as it is very less magnitude. Therefore after neglecting voltage drop from the equation (6) the estimated change in stator flux can be written as in (7) by assuming sampling time period, ΔT_s is very small. Similarly the change torque equation is expressed as in (8).

$$\vec{\Psi}_s = \int (\vec{V}_s - R_s \vec{I}_s)\, dt. \tag{6}$$

$$\Delta\vec{\Psi}_s = \vec{V}_s\, \Delta T_s \tag{7}$$

$$\Delta T_e = \frac{3}{2}\left(\frac{P}{2}\right)\frac{L_m}{\sigma L_s L_r}\left|\vec{\Psi}_r\right|\left|\vec{\Psi}_s + \Delta\vec{\Psi}_s\right| \sin\Delta\delta_\Psi \tag{8}$$

The stator flux vector of the induction motor moves in the direction of voltage and its change is rapidly affected by voltage vector as in (7). The rotor flux vector movement is considerably slower than the stator flux vector due to its higher rotor time constant. The quick movement of stator flux vector also causes change in torque angle δ_Ψ, hence increase or decrease in flux and torque is accountable merely by the stator voltage. The quick change in electromagnetic torque from (8) is mainly affected by the $\Delta\delta_\Psi$ in the desired direction. The stator flux magnitude also changes in proportion to the voltage and it is oriented in the same direction of the stator voltage vector. Hence, here inverter switching with appropriate active voltage vector is provided with the help of standard look-up table and therefore this method control is called as DTC [1], [2], [3], [4]. The step by step application of appropriate voltage vector changes the flux and torque then they are compared with reference flux/torque magnitudes. Thus in DTC, error infor-

mation of estimated toque in (5) and estimated stator flux in (6) are used in hysteresis controllers as shown in the Fig. 1(a) and Fig. 1(b). The control scheme for inverter switching is obtained based on increase, decrease or no change in the torque and flux magnitudes. The stator flux and torque are regulated within prescribed tolerances and the proper switching voltage vectors are selected as per the switching table shown in Table – I, where torque hysteresis controller band tolerances are defined as

$$|T_{em}| < |T_{em}^{ref}| - |\Delta T_{BW}| \quad \Rightarrow \quad D_T = 1, \qquad (9)$$

$$-|\Delta T_{BW}| < \{|T_{em}^{ref}| - |T_{em}|\} \leq |\Delta T_{BW}| \quad \Rightarrow \quad D_T = 0, \qquad (10)$$

$$|T_{em}| > |T_{em}^{ref}| - |\Delta T_{BW}| \quad \Rightarrow \quad D_T = -1 \qquad (11)$$

For flux the hysteresis controller band tolerances are defined as

$$|\Psi_s| \leq |\Psi_s^{ref}| - |\Delta\Psi_{BW}| \quad \Rightarrow \quad D_\Psi = 1 \qquad (12)$$

$$|\Psi_s| \geq |\Psi_s^{ref}| - |\Delta\Psi_{BW}| \quad \Rightarrow \quad D_\Psi = 0 \qquad (13)$$

The block diagram of conventional DTC of induction motor is shown in the Fig. 2, it consists of mainly torque flux estimation, torque estimation, flux control, torque control and switching table blocks. The PI controller is used in the outer loop of the drive to generate reference torque, whereas flux reference is manually given as shown in the Fig. 2. The D_T and D_Ψ signals are updated from the hysteresis controllers, then these are finally used to select required voltage vector implemented in the look-table [2], [5]. The three phase voltage source PWM inverter is used to operate the induction motor.

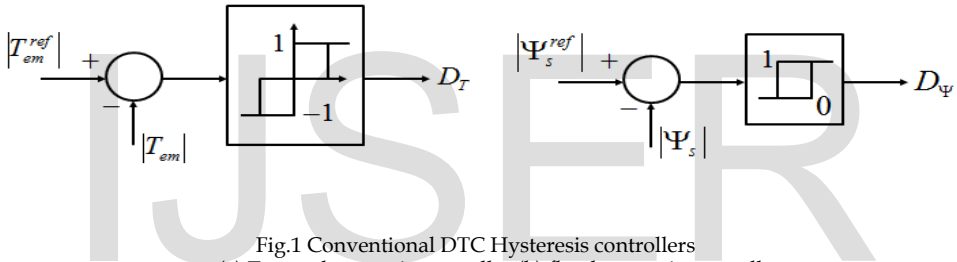

Fig.1 Conventional DTC Hysteresis controllers
(a) Torque hysteresis controller (b) flux hysteresis controller

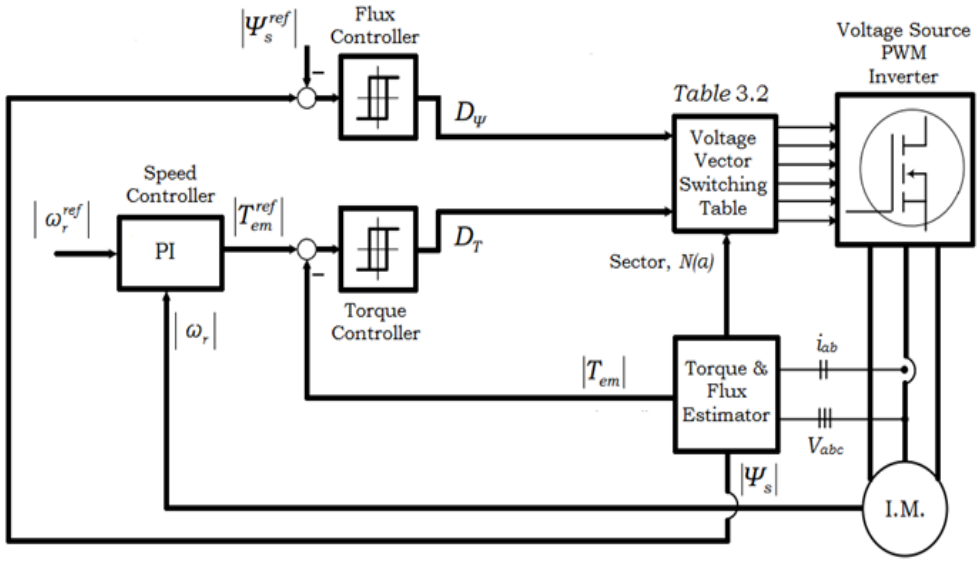

Fig.2 Block diagram of conventional induction motor drive

TABLE – I
VOLATGE VECTOR LOOKUP TABLE / SWITCHING TABLE FOR CONVENTIONAL DTC

D_Ψ	D_T	Sector 1	Sector 2	Sector 3	Sector 4	Sector 5	Sector 6
1	1	$\overline{V}_2$ (110)	$\overline{V}_3$ (010)	$\overline{V}_4$ (011)	$\overline{V}_5$ (001)	$\overline{V}_6$ (101)	$\overline{V}_7$ (111)
	0	$\overline{V}_7$ (111)	$\overline{V}_0$ (000)	$\overline{V}_7$ (111)	$\overline{V}_0$ (000)	$\overline{V}_7$ (111)	$\overline{V}_0$ (000)
	-1	$\overline{V}_6$ (101)	$\overline{V}_1$ (100)	$\overline{V}_2$ (110)	$\overline{V}_3$ (010)	$\overline{V}_4$ (011)	$\overline{V}_5$ (001)
0	1	$\overline{V}_3$ (010)	$\overline{V}_4$ (011)	$\overline{V}_5$ (001)	$\overline{V}_6$ (101)	$\overline{V}_1$ (100)	$\overline{V}_2$ (110)
	0	$\overline{V}_0$ (000)	$\overline{V}_7$ (111)	$\overline{V}_0$ (000)	$\overline{V}_7$ (111)	$\overline{V}_0$ (000)	$\overline{V}_7$ (111)
	-1	$\overline{V}_5$ (001)	$\overline{V}_6$ (101)	$\overline{V}_1$ (100)	$\overline{V}_2$ (110)	$\overline{V}_3$ (010)	$\overline{V}_4$ (011)

TABLE –II
SWITCHING TABLE FOR BUS CLAMPED DTC STRATEGY
(DERIVED FROM TWO LEVEL TORQUE CONTROL)

D_Ψ / D_T	+1 / +1	+1 / –1	0 / +1	0 / –1	Clamped Phase	DC Bus
Sector I	V_2	V_0 / V_1	V_3	V_0	c	$-V_{dc}$
Sector II	V_3	V_7 / V_2	V_4	V_7	b	$+V_{dc}$
Sector III	V_4	V_0 / V_3	V_5	V_0	a	$-V_{dc}$
Sector IV	V_5	V_7 / V_4	V_6	V_7	c	$+V_{dc}$
Sector V	V_6	V_0 / V_5	V_1	V_0	b	$-V_{dc}$
Sector VI	V_1	V_7 / V_6	V_2	V_7	a	$+V_{dc}$

5 BUS CLAMPED DIRECT TORQUE CONTROL SCHEME

The voltage vectors selection in conventional DTC method is mainly based on torque and flux control and their switching sequences are shown Table - I. Suppose, inverter switching in sector – I merely comprises of active voltage space vectors, V_2, V_6, V_3 and V_5 for all conditions of D_Ψ and D_T eliminating no change command operation in the torque control. Here, the zero vector switching can be ignored to circumvent the drawback of retardation of flux leading to high ripple. This makes reduced switching table which accomplishes only active vectors in the inverter switching. The switching states between any two voltage vectors are redefined to achieve bus clamped space vector modulation which is slightly alters conventional DTC operation, where switching makes pole voltage of one of the phase is either $+V_{dc}$ or $-V_{dc}$ as constant up to some duration in every switching intervals [17]. That is periodically any one of the inverter phase is switched to be clamped to DC voltage bus. The process of bus clamping DTC is given in [17] and modified switching tables are derived for both clockwise and anti-clock wise rotations of induction motor operation. Suppose in the sector – I, the switching voltage vectors in bus clamped based DTC having flux and torque commands of $D_\Psi = 0$, $D_T = 1$ and $D_\Psi = 1$, $D_T = -1$ is completely required to be redefined and here, every sector is considered to have 300 in the implementation. The switching table for bus clamped DTC is shown in the Table – II. The V_0 / V_1 entry in Table – II means that, in sector – I the voltage vector V_0 is switched for the first 30^0 sub-sector and in the second 30^0 sub-sector it is switched with voltage vector V_1.

6 FOUR LEVEL HYSTERESIS BASED BUS CLAMPED DTC

In the DTC, inverter has been controlled with two level torque and flux controllers in which actual flux and torque response has not been exactly equal to their reference values, since no inverter voltage vector is desirably produce flux and flux. Therefore conventional DTC or bus clamped DTC suffers mainly from higher flux and torque ripples. The solution to circumvent this problem is increasing number of hysteresis band tolerances, by which inverter switching can be finitely adopted by adjusting active voltage vector and null voltage vector switching combinations. A multiple torque hysteresis band control is proposed for bus clamped DTC in which

torque control is adopted with four band tolerances. The flux is controlled usually with two tolerances of band settings for hysteresis controllers [12]. The torque control is synthesized such that the digitization signal, D_T should consists of +2, +1, –1 and –2 and flux control synthesized +1 and 0 merely, where torque hysteresis controller band tolerances are defined as

$$|T_{em}| < |T_{em}^{ref}| - |\Delta T_{BW\,2}| \quad \Rightarrow \quad D_T = +2\,, \qquad (14)$$

$$0 < \left\{|T_{em}^{ref}| - |T_{em}|\right\} \le |\Delta T_{BW\,1}| \quad \Rightarrow \quad D_T = +1 \qquad (15)$$

$$-|\Delta T_{BW\,1}| \le \left\{|T_{em}^{ref}| - |T_{em}|\right\} < 0 \quad \Rightarrow \quad D_T = -1 \qquad (16)$$

$$|T_{em}| > |T_{em}^{ref}| - |\Delta T_{BW\,2}| \quad \Rightarrow \quad D_T = -2\,, \qquad (17)$$

The four level toque hysteresis controllers are operated with duty cycle control, where the duty cycle is estimated which gives active time of operation of particular voltage vector which is selected from the switching table. Here, the duty cycle is desirably computed, since the same voltage vectors has to be applied when, $D_\Psi = +1$, $D_T = +2$ and $D_\Psi = +1$, $D_T = +1$ in the sector – I. Therefore, it is desired that, in sector – I if $D_\Psi = +1$ and $D_T = +2$ then V_2 is operated with 100 % duty cycle period of 'd ', when $D_\Psi = +1$ and $D_T = +1$ then is 50% of duty time 'd ' is operated with V_2 and the remaining 50% of duty cycle period V_0 is selected. The duty cycle period 'd ' is computed by applying the torque ripple minimization criterion which is expressed as [4]

$$d = \frac{1}{T_S}\frac{2\left\{|T_{em}^{ref}| - |T_{em}|\right\}}{2S_{12} - S_{00}} \qquad (18)$$

where, S_{12} is switching time of second active vector, S_{00} is zero voltage vector switching time and T_S is total switching time.

The switching table for bus clamping DTC with four level hysteresis torque controller is obtained by identifying switching states such that the same phases are to be clamped as shown the Table – II. So far, the selection of V_2 and V_0 assures bus clamping, whereas in the remaining cases also secures to have bus clamping. Similar to the process as applied in bus clamped DTC, when flux and torque commands are equal to $D_\Psi = +1$ and $D_T = +2$ in sector – I then both torque and flux is increased which can be accomplished by switching V_2 voltage vector. When $D_\Psi = +1$ and $D_T = +1$ then same voltage V_2 is applied such that duty cycle control is asserted therefore the switching of V_2 / V_0 is carried by sharing 50% duty cycle allocation time to each of them. The new voltage vectors V_1 / V_0 are used when $D_\Psi = +1$, $D_T = -1$ and $D_\Psi = +1$, $D_T = -2$ to have bus clamping action to control flux and torque in this region. The inverter switching when $D_\Psi = 0$ and $D_T = +2$ case operation is same as conventional DTC operation corresponding to achieve decrease in flux and decrease in torque and $D_\Psi = 0$ and $D_T = +1$ is also equal to the operation $D_\Psi = 0$ and $D_T = +2$ as therefore for both of these cases voltage vector V_3 is used. When $D_\Psi = 0, D_T = -1$ and $D_\Psi = 0, D_T = -2$ the torque and flux control decrease is asserted by zero voltage vector selection, hence V_7 / V_0 are appropriately chosen to ensure the bus clamping. Thus the selection of these voltage vectors clamps c-phase of the inverter to V_{-dc} bus. The selection of voltage vectors of sectors 2 to 6 is similarly obtained. The Table – III shows the switching table for four level bus clamped DTC.

TABLE – III
SWITCHING TABLE FOR FOUR LEVEL TORQUE HYSTERESIS BAND BASED BUS CLAMPED DTC METHOD

D_Ψ / D_T	+1 / +2	+1 / +1	+1 / –1	+1 / –2	0 / +2	0 / +1	0 / –1	0 / –2	Clamped Phase	DC Bus
Sector I	V_2	V_2 / V_0	V_1 / V_0	V_1 / V_0	V_3	V_3	V_0	V_7	c	$-V_{dc}$
Sector II	V_3	V_3 / V_7	V_2 / V_7	V_2 / V_7	V_4	V_4	V_7	V_0	b	$+V_{dc}$
Sector III	V_4	V_4 / V_0	V_3 / V_0	V_3 / V_0	V_5	V_5	V_0	V_7	a	$-V_{dc}$
Sector IV	V_5	V_5 / V_7	V_4 / V_7	V_4 / V_7	V_6	V_6	V_7	V_0	c	$+V_{dc}$
Sector V	V_6	V_6 / V_0	V_5 / V_0	V_5 / V_0	V_1	V_1	V_0	V_7	b	$-V_{dc}$
Sector VI	V_1	V_1 / V_7	V_6 / V_7	V_6 / V_7	V_2	V_2	V_7	V_0	a	$+V_{dc}$

6 SIMULATION RESULTS

The performance conventional DTC, two level torque hysteresis torque controlled bus clamped DTC and proposed four level hysteresis torque controlled bus clamped DTC are verified with simulation results. The rating and parameters of three phase induction motor is shown in Appendix. The simulation results signifying bus clamping operation and non-bus clamping operation can be verified through pole voltages shown in Fig. 3. The simulation results of sector computation for conventional DTC (CDTC), two level torque hysteresis torque controlled bus clamped DTC (2L THB BCDTC) and four level hysteresis torque controlled bus clamped DTC (4L THB BCDTC) is shown in Fig. 3(a). The Fig. 3(b), Fig. 3(c) and Fig. 3(d) shows simulation results of pole voltages of a-phase, b-phase and c-phase of CDTC, 2L THB BCDTC and 4L THB BCDTC induction motor drive. It observed that clamping of pole voltages is more in 4L THB BCDTC compared to 2L THB BCDTC but there is no clamping for CDTC.

The Fig. 4(a) shows simulation results of phase voltage of CDTC, 2L THB BCDTC and 4L THB BCDTC to an induction motor drive and The individual response of one phase voltage of CDTC is shown in Fig. 4(a-1), for 2L THB BCDTC response is shown in Fig. 4(a-2) and in the case of 4L THB BCDTC result is shown in Fig. 4(a-3). The simulation results of phase currents of CDTC, 2L THB BCDTC and 4L THB BCDTC is shown in the Fig. 4(b). The phase stator current of CDTC has been shown in Fig. 4 (b-1), 2L THB BCDTC shown in Fig. 4 (b-2) and for 4L THB BCDTC shown in Fig. 4 (b-3). It is observed that the current distortion is less in the case of proposed 4L THB BCDTC induction motor drive. The Fig.5 shows frequency spectrum of total harmonic distortion (THD) obtained for stator current in the case of CDTC induction motor drive, it is observed that current THD of stator current is 12.58 %. Fig. 6 shows current harmonic distortion in the case with 2L THB BCDTC method, here it is observed that the distortion is 10.58 %. In case of 4L THB BCDTC method harmonic distortion plot is shown in Fig. 7, it is noticed that the distortion of current is 7.5 %. Thus distortion is marginally reduced in the proposed method.

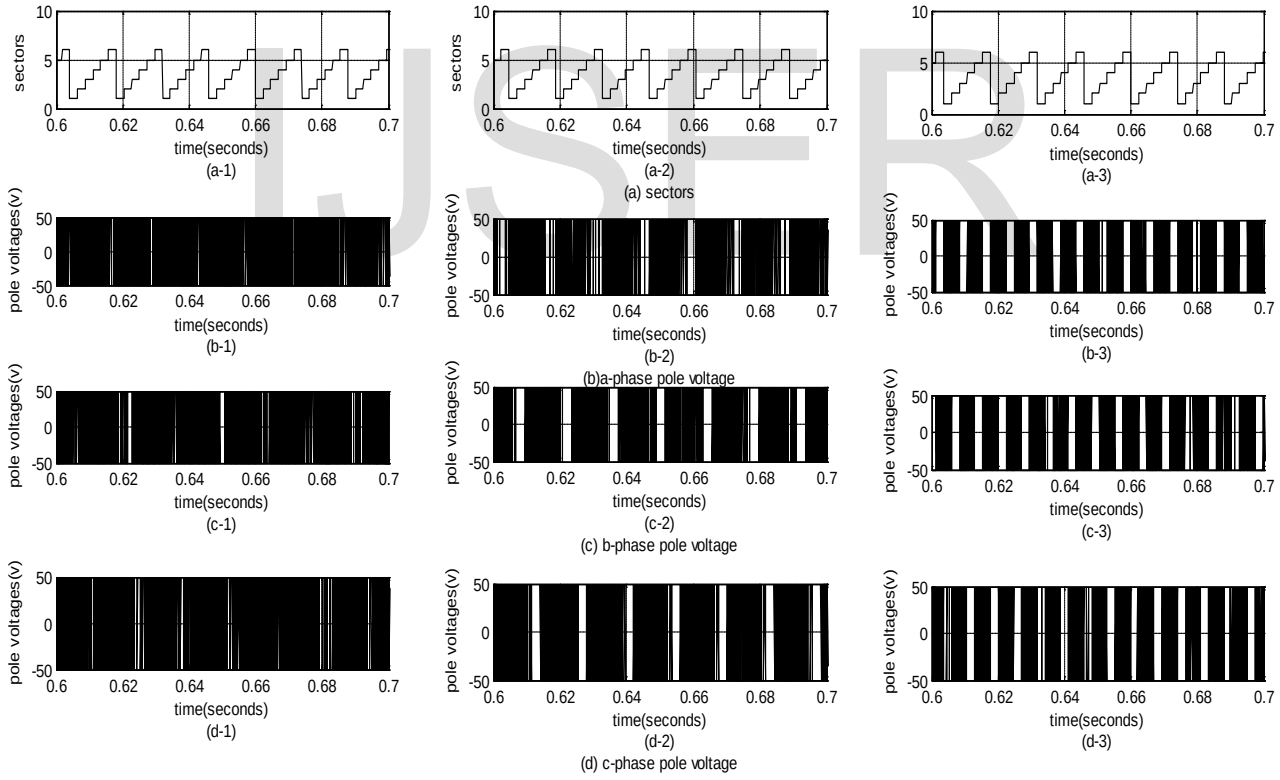

Fig.3 Simulated results of conventional DTC, two level torque hysteresis band bus clamped DTC and four level torque hysteresis band bus clamped DTC for reference speed ref. = 157 rad / sec and load torque = 0.7 N-m. (a) sectors locus, (b) a-phase pole voltage, (c) b- phase pole voltage, (c) c- phase pole voltage.

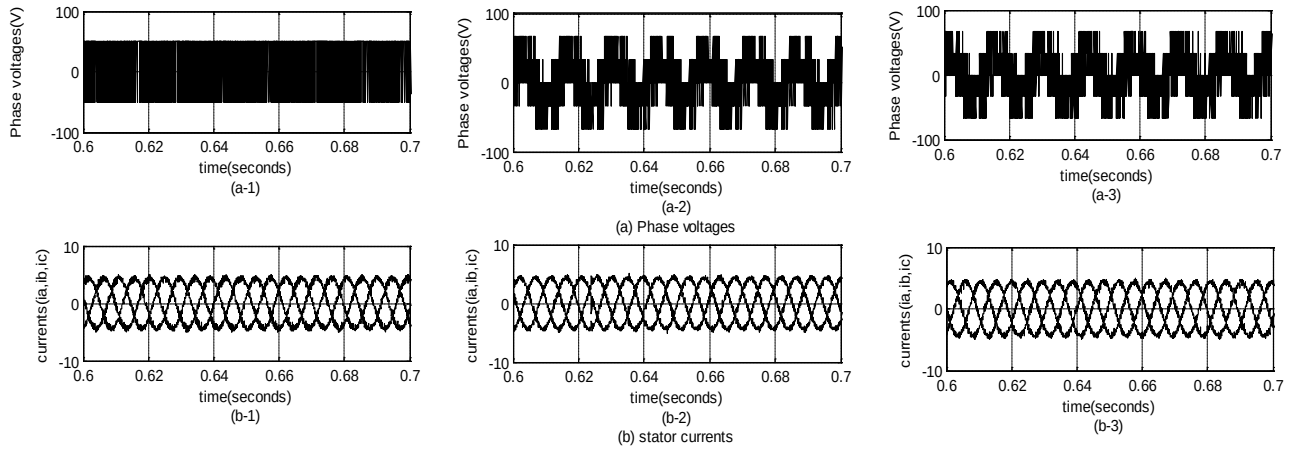

Fig.4 Simulated results of conventional DTC, two level torque hysteresis band bus clamped DTC and four level torque hysteresis band bus clamped DTC for speed ref. =157 rad / sec and load torque = 0.7 N-m.(a) phase voltage of phase a (b) stator currents.

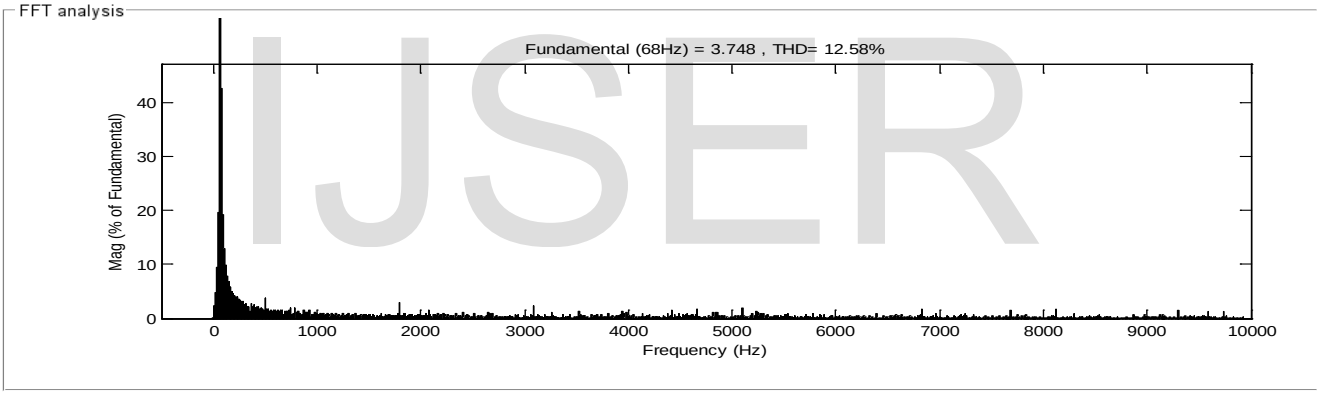

Fig.5 Current frequency spectrum of conventional DTC induction motor drive

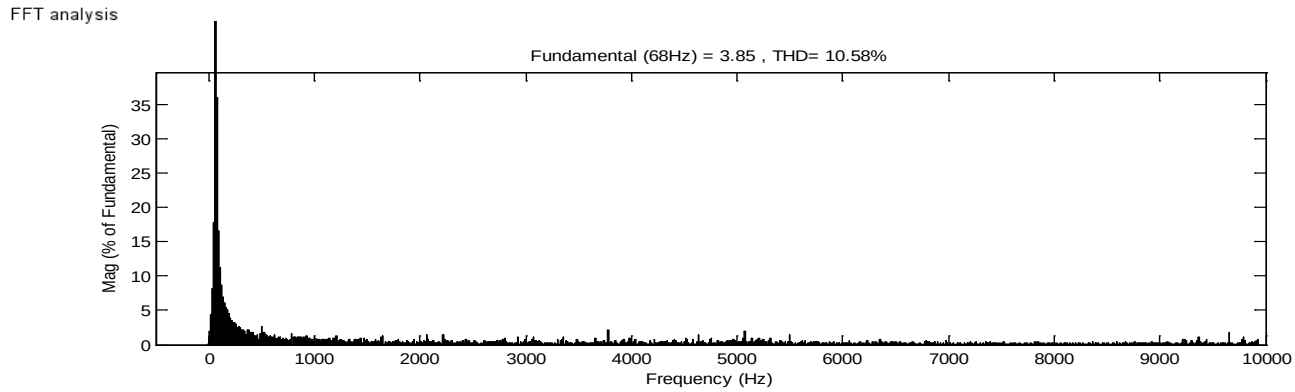

Fig.6 Current frequency spectrum of two level hysteresis band bus clamped DTC induction motor drive

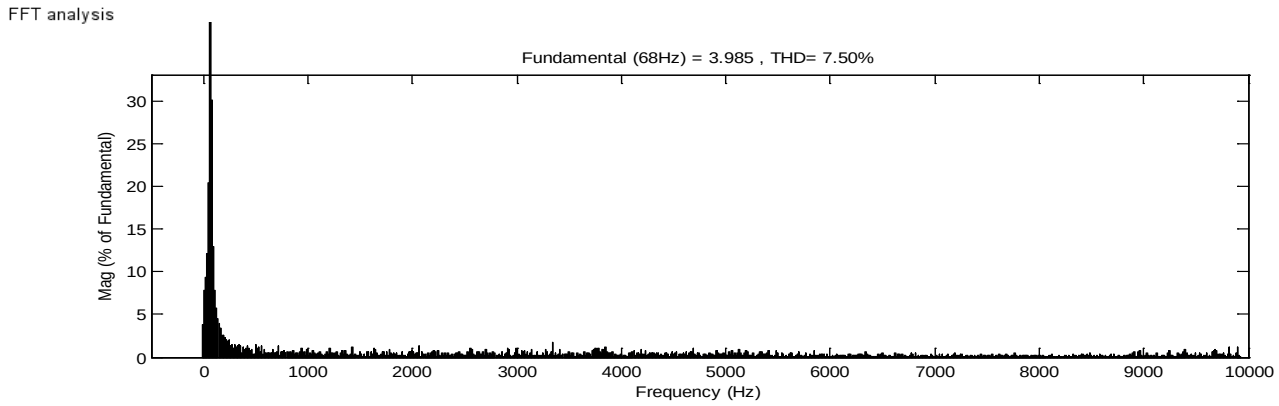

Fig.7 Current frequency spectrum of four level torque hysteresis band bus clamped DTC induction motor drive

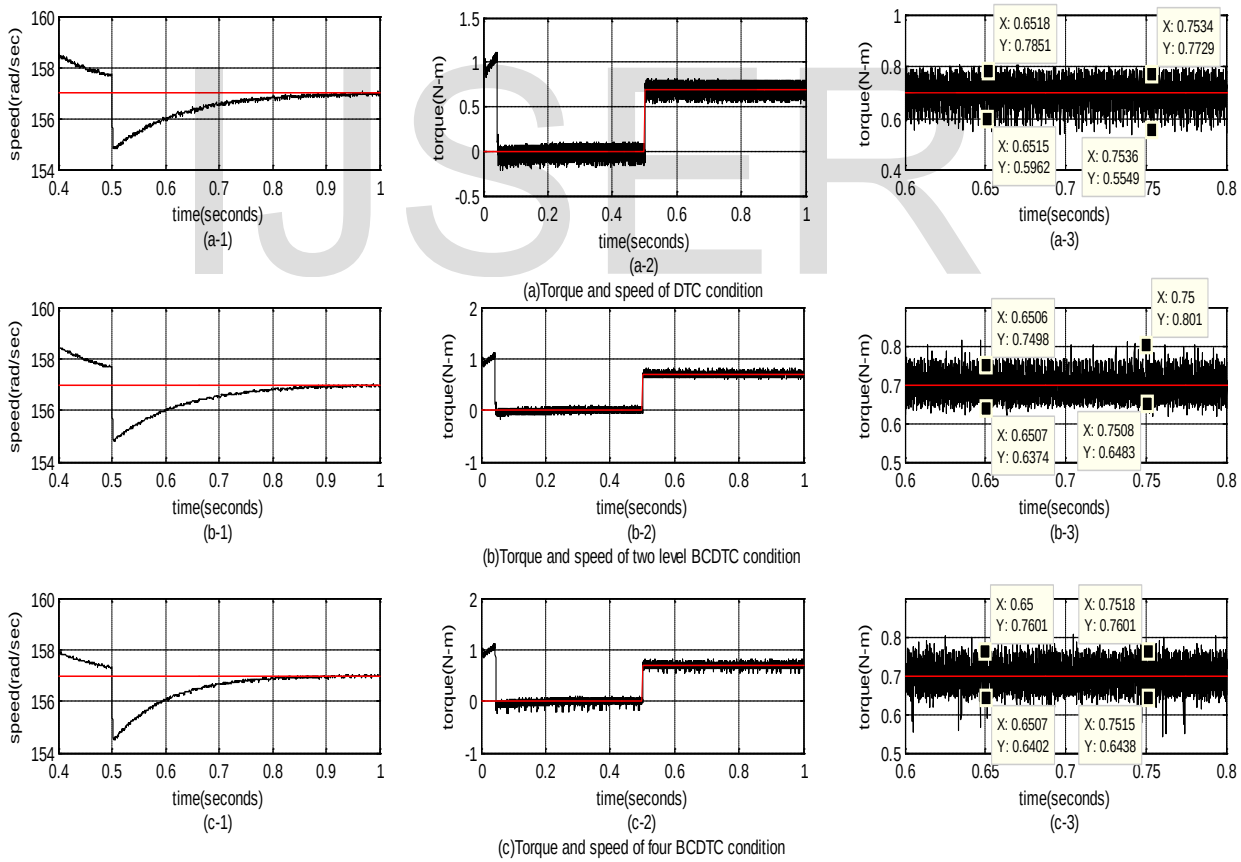

Fig.8 Simulation results of conventional DTC, two level torque hysteresis band bus clamped DTC and four level torque hysteresis band bus clamped DTC speed ref. =157 rad / sec and load torque = 0.7 N-m.(a) Torque and speed in ST-DTC strategy (b) Torque and speed in Two level torque hysteresis band bus clamped DTC strategy (c) Torque and speed in four level torque hysteresis band bus clamped DTC strategy

ventional CDTC induction motor drive. Fig. 8(a-1), actually

shows zoomed speed response, by which it is observed that under sudden applied full load of 0.7 N-m the drop in speed is around 2.5 rad/sec. Fig. 8(b) and Fig. 8(c) shows speed and torque simulation results of 2L THB BCDTC and 4L THB BCDTC induction motor drive respectively. Fig. 8(b-1) and 8(c-1) illustrates zoomed speed responses of 2L THB BCDTC and 4L THB BCDTC it is observed that, the speed drop on the both of these are around 2 rad/sec. Based on the observations three cases peed responses on the sudden application of step change in load, it is conferred that the dynamic speed characteristics of 2L THB BCDTC and 4L THB BCDTC methods are similar to the CDTC method.

TABLE – IV
COMPARATIVE PERFORMANCE RESULTS

Performance parameter	DTC Strategy		
	CDTC	**2L THB BCDTC**	**4L THB BCDTC**
When speed ref. =157 rad / sec and load torque = 0.7 N-m.			
Torque ripple	28.5%	23%	17%
Flux ripple	8.5%	7.8%	6.75%
Current THD	12.58%	10.58%	7.5%
When speed ref. =157 rad / sec and load torque = 0.35 N-m.			
Torque ripple	58.9%	37%	33.5%
Flux ripple	9.85%	9.05%	8.25%
Current THD	26.31%	23.99%	21.64%
When speed ref. = 30rad / sec and load torque = 0.7 N-m.			
Torque ripple	32%	22.5%	19.5%
Flux ripple	9.65%	7.55%	6.8%
Current THD	77.16%	71%	71%
When speed ref. = 30 rad / sec and load torque = 0.35 N-m.			
Torque ripple	65.5%	32.5%	25%
Flux ripple	8.25%	6.65%	6.5%
Current THD	98%	93%	92%

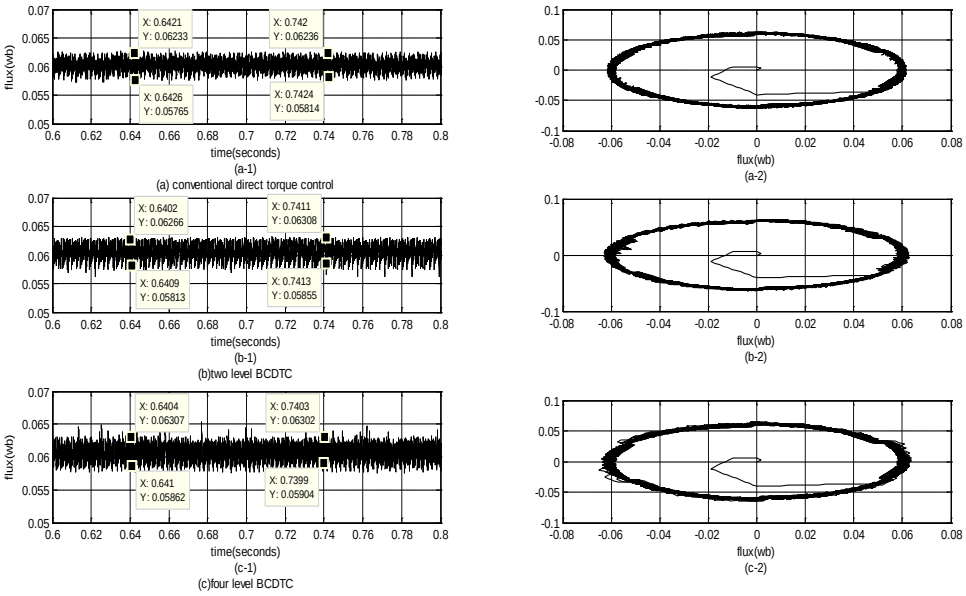

Fig.9 Simulated resul;t of ST-DTC, two level torque hysteresis band bus clamped DTC and four level torque hysteresis band bus clamped DTC for speed ref. =157 rad / sec and load torque = 0.7 N-m. (a) flux response in conventional DTC strategy (b) flux response for two level torque hysteresis band bus clamped DTC strategy (c) flux response for four level torque hysteresis band bus clamped DTC strategy

Fig. 8(a-2) shows the torque response of CDTC with step change in full load of 0.7 N-m applied at 0.5 sec simulation

time, its zoomed response is shown in Fig. 8(a-3). It is observed that, by using data tips marked on this figure the calculated torque ripple based on is 28.5%. Similarly, the torque ripple is obtained for 2L THB BCDTC and 4L THB BCDTC methods and from the zoomed torque responses shown in the Fig. 8(b-3) and Fig. 8(c-3). The calculated torque ripple in the case of 2L THB BCDTC method is 23%, whereas the torque ripple for 4L THB BCDTC is 16.5%. It is observed that the torque ripple in the case of proposed 4L THB BCDTC strategy is less compared with CDTC and 2L THB BCDTC methods. The dynamic speed response is same for all the strategies. The Fig. 9(a) shows flux simulation results of CDTC induction motor drive. The zoomed flux response is shown in the Fig. 9(a-1) and flux locus is shown in Fig. 9(a-2). It is observed that, by using data tips marked on this figure and flux ripple is 8.25%. The Fig. 9(b) and Fig. 9(c) shows flux simulation results of 2L THB BCDTC and 4L THB BCDTC induction motor drive respectively. The Fig. 9(b-1) and 9(c-1) shows zoomed flux response of 2L THB BCDTC and 4L THB BCDTC. The flux locus of 2L THB BCDTC and 4L THB BCDTC is in Fig. 9(b-2) and 9(c-2). The calculated flux ripple in the case of 2L THB BCDTC is 6.65% and in the case of 4L THB BCDTC method flux ripple is 6.55%. Reduction of flux ripple in case of 4L THB BCDTC method is more less is same as 2L THB BCDTC, however torque ripple is marginally reduced. The comparative performance results CDTC, 2L-THB BCDTC and 4L-THB BCDTC methods at rated speed and low speed cases with full load and half full load conditions are shown in the Table – IV.

6 Conclusions

In this paper four level torque hysteresis controller based bus clamped DTC of induction motor is presented, the selection of voltage vectors for higher level hysteresis band controller can be adopted by adjusting duty cycle with insertion of zero vectors/ non zero vectors without compromising dynamic response. The simulation results of two level torque hysteresis band bus clamped DTC and four level torque hysteresis band bus clamped DTC of Induction motor are presented. The proposed four level torque hysteresis band bus clamped DTC of induction motor reduces torque ripple marginally and current harmonic distortion is also well reduced. The dynamic speed response of the proposed method is most satisfactory as same as the basic methods and thus this method can well adopted in torque pulsations sensitive applications.

Appendix

Fractional h.p., Induction Motor parameters:

Rating: P = 120 W, Vr = 30 V, 3 Ph-AC, f = 120 Hz, Ir = 6 A, p = 4.

Parameters: RS = 0.896 Ω, Lls = 1.94 mH, Rr = 1.82 Ω, Llr = 2.45 mH, Lm = 69.3 mH.

References

[1] I. Takahashi and T. Noguchi, "A new quick-response and high-efficiency control strategy of an induction motor," IEEE Trans. Ind. Appl., Vol. 22, No.5, pp. 820-827,1986.

[2] T. Noguchi, M. Yamamoto, S. Kondo and I. Takahashi, "High frequency switching operation of PWM inverter for direct torque control of induction motor", Conference Record of the lndustly Applications Annual Meeting IAS'97, Vol. I, pp. 775-780, 1997.

[3] P. Marino, M. D. Incecco and N.Visciano, "A comparison of direct torque control methodologies for induction motor," IEEE Porto Power Tech procedings, vol. 2, 6 pp., 2001.

[4] Y. Zhang and J. Zhu, "A novel duty cycle control strategy to reduce both torque and flux ripples for DTC of permanent magnet synchronous motor drives with switching frequency reduction", IEEE Trans. Power Electronics, Vol. 26, No. 10, pp. 30553067, 2011.

[5] P. Zhu, Y.Kang and J.Chen, "Improve direct torque control performance of induction motor with duty ratio modulation", IEEE International Electric Machines and Drives Conference, vol.2,pages: 994 – 998, 2003.

[6] Buja, G.S., and Kazmierkowski, M. P., "Direct torque control of PWM inverter-fed AC motors – a survey," IEEE Trans. Ind. Appl., Vol.51, pp.744-757, 2004.

[7] N. Rumzi, N. Idris, A.H.M. Yatim, "Direct torque control of induction motors with constant switching frequency and reduced torque ripple", IEEE Trans. on Industry Applications, vol. 51, no. 4, pp. 758-767, Aug. 2004.

[8] N. Rumzi, N. Idris, C.L. Toh, M.E.Elbuluk, "A new torque and flux controller for direct torque control of induction motor", IEEE Trans. on Industry Applications, vol. 42, no. 6, pp. 1358-1366, Nov./Dec. 2006.

[9] Yen-Shin Lai, Wen-Ke Wang, and Yen-Chang. Chen, "Novel switching techniques for reducing the speed ripple of AC drives with direct torque control," IEEE Trans. Ind. Electron., vol. 51, no. 4, pp. 768–775, Aug. 2004.

[10] J.K. Kang and S.K.Sul, "New direct torque control of induction motor for minimum torque ripple and constant switching frequency", IEEE Trans. Ind. Appl., vol.35, no.5, pp.1076–1082, Sep./Oct.1999.

[11] K. K. Shyu, J. K. Lin, V.T. Pham, M. J. Yang, and T.W. Wang, "Global minimum torque ripple design for direct torque control of induction motor drives," IEEE Trans. Ind. Electron., vol. 57, no. 9, pp. 3148–3156, Sep. 2010.

[12] Kanungo Barada Mohanty, "A Direct Torque Controlled Induction Motor with Variable Hysteresis Band," 11th International Conference on Computer Modelling and Simulation. 2009.

[13] A. Tripathi, A. M. Khambadkone, and S. K. Panda, "Torque ripple analysis and dynamic performance of a space vector modulation based control method for AC-drives," IEEE Trans. Power Electron., vol. 20, no. 2, pp. 485–492, Mar. 2005.

[14] Pandya S.N., Chatterjee J.K., "Torque Ripple Reduction in Direct Torque Control based Induction Motor Drive using Novel Optimal Controller Design Technique., Joint International Conference on Power Electronics, Drives and Energy Systems (PEDES) & 2010 Power India, pp. 1-7.

[15] A. Jidin, N . R. N. Idris, A. H. M. Yatim, T. Sutikno, and M. E. Elbuluk, "Simple dynamic over modulation strategy for fast torque control in DTC of induction machines with constant-switching-frequency controller", IEEE Trans. Ind. Appl., vol. 47, no. 5, pp. 2283-2291, 2011.

[16] B. Bouzidi, B. El Badsi, and A. Masmoudi, "Investigation of the performance of a DTC strategy dedicated to the control of B4 fed induction motor drives," Computation and Mathematics in Electrical and Electronic Engineering (COMPEL), vol. 31, no. 1, pp. 224–236, 2012.

[17] B. EI Badsi, B. Bouzidi, and A. Masmoudi, "Bus-clamping based DTC: an attempt to reduce harmonic distortion and switching losses", IEEE Trans. Ind. Electron., vol. 60, no. 3, pp. 873-884, 2013.

[18] V. S. S. Pavan Kumar Hari and G. Narayanan, "Theoretical and experimental evaluation of pulsating torque produced by induction motor drives controlled with advanced bus-clamping pulse width modulation," IEEE Trans. Ind. Electron., vol. 63, no. 3, pp. 1404–1413, Mar. 2016.

[19] B. Ozpineci and L.M. Tolbert , "Simulink Implementation of Induction Machine Model-A Modular Approach," in Proceedings of the IEEE International Electric Machines and Drives Conference (IEMDC), 2003, pp. 728-734.

[20] P.C. Krause, O. Wasynczuk, and S.D. Sudhoff, Analysis of Electric Machinery, IEEE Press, NY: 1995.